

# **$B$ -meson production in $p\bar{p}$ collisions at Tevatron with $k_T$ -factorization**

S.P. Baranov<sup>1</sup>

*P.N. Lebedev Institute of Physics,  
117924 Moscow, Russia*

A.V. Lipatov<sup>2</sup>

*Physical Department, M.V. Lomonosov Moscow State University,  
119992 Moscow, Russia*

N.P. Zotov<sup>3</sup>

*D.V. Skobeltsyn Institute of Nuclear Physics,  
M.V. Lomonosov Moscow State University,  
119992 Moscow, Russia*

## **Abstract**

In the framework of the  $k_T$ -factorization QCD approach we consider the production of  $b$  quark pairs in  $p\bar{p}$  collisions at the Fermilab Tevatron. We investigate the dependence of the  $b$  quark,  $B$  meson and decay muon differential cross sections on the different forms of unintegrated gluon distributions. The analysis also covers the azimuthal correlations between the  $b$  and  $\bar{b}$  quarks and their decay muons. Our theoretical results agree well with recent data taken by the DØ and CDF collaborations at Tevatron. Finally, we present our predictions for muon-muon and muon-jet cross sections at the Tevatron and CERN LHC conditions.

## **1 Introduction**

Recently DØ and CDF collaborations have reported new experimental data [1–5] on the  $b$ -flavor production at the Tevatron. These data are found to be about a factor of two or

---

<sup>1</sup>E-mail: baranov@sci.lebedev.ru

<sup>2</sup>E-mail: lipatov@theory.sinp.msu.ru

<sup>3</sup>E-mail: zotov@theory.sinp.msu.ru

more larger than the predictions of perturbation theory (pQCD) at next-to-leading order (NLO) [1–6]. Therefore, it would be certainly reasonable to try a different way.

At the energies of modern colliders (such as Tevatron and LHC), heavy quark and quarkonium production processes belong to the class of the so called semihard processes [7–10]. In these processes, by the definition, the hard scattering scale  $\mu \sim m_Q$  is much larger than the QCD parameter  $\Lambda_{\text{QCD}}$ , but, on the other hand, it is much smaller than the total center-of-mass energy:  $\Lambda_{\text{QCD}} \ll \mu \ll \sqrt{s}$ . The last condition means that these processes occur in the small  $x$  region,  $x \simeq m_Q/\sqrt{s} \ll 1$ , where the contributions of the "large logarithms" to the evolution of gluon densities are known to become rather important. It is known also that in the small  $x$  region it becomes necessary to take into account the dependence of the subprocess cross sections and gluon structure functions on the gluon transverse momentum  $k_T$  [7–10]. Therefore, the  $k_T$ -factorization (or semihard) approach provides a more suitable ground for the calculations than the ordinary parton model.

The  $k_T$ -factorization approach is based on the Balitsky-Fadin-Kuraev-Lipatov (BFKL) [11] evolution equation for gluon densities. The resummation of the terms  $\alpha_S^n \ln^n(\mu^2/\Lambda_{\text{QCD}}^2)$ ,  $\alpha_S^n \ln^n(\mu^2/\Lambda_{\text{QCD}}^2) \ln^n(1/x)$  and  $\alpha_S^n \ln^n(1/x)$  leads to the so called unintegrated ( $q_T$ -dependent) gluon distributions  $\Phi(x, q_T^2, \mu^2)$  which determine the probability to find a gluon carrying the longitudinal momentum fraction  $x$  and transverse momentum  $q_T$  at the probing scale  $\mu^2$ . In contrast with the usual parton model, the unintegrated gluon distributions have to be convoluted with off-mass-shell matrix elements corresponding to the relevant partonic subprocesses [7–10]. In the off-mass-shell matrix elements, the virtual gluon polarization tensor is taken in the form [7–10]:

$$L^{\mu\nu} = \frac{q_T^\mu q_T^\nu}{q_T^2}. \quad (1)$$

The  $b$ -flavor production at the Tevatron in the  $k_T$ -factorization approach was considered earlier in [8, 12–17]. However, the off-shell matrix elements of hard partonic subprocess presented in [8] contain some misprints. Also, the results obtained in the paper [16] do not agree with other results [12–15].

In our previous paper [17], we analyzed the  $p_T$  distribution of the produced  $b$ -quarks (presented in the form of integrated cross sections). Our results agree well with DØ [5] and CDF [3] experimental data. Also, we found that our off-shell matrix elements for partonic subprocess coincide with the ones presented in Ref. [9].

Here, we use the  $k_T$ -factorization approach for a more detailed analysis of the experimental data [1–5]. We inspect the dependence of the  $b$  quark,  $B$  meson and decay muon cross sections on the different forms of the unintegrated gluon distributions. The analysis also covers the azimuthal correlations between the  $b$  and  $\bar{b}$  quarks and their decay muons. Special attention is paid to the role of the unintegrated gluon distributions which has been applied earlier in our previous papers [17–22]. In addition, we present our predictions for muon-muon and muon-jet cross sections at the Tevatron and CERN LHC conditions.

The outline of this paper is as follows. In Section 2 we present the analytical expressions for the total and differential cross sections of the inclusive heavy quark production in the  $k_T$ -factorization approach and describe the unintegrated gluon distributions which we use in our calculations. In Section 3 we present the numerical results of our calculations and compare them with the DØ [4, 5] and CDF [1–3] data. Finally, in Section 4, we give some conclusions.

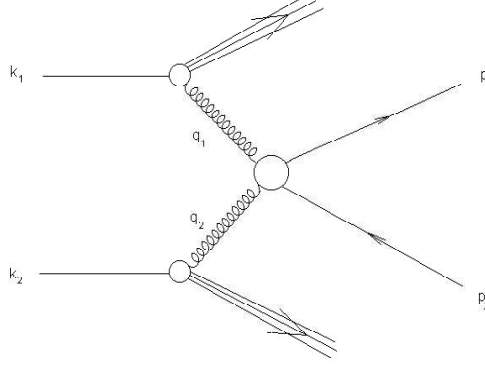


Figure 1: Diagram for the  $p\bar{p} \rightarrow b\bar{b} X$  process.

## 2 Theoretical framework

In this section we present the expressions for the inclusive heavy quark production total and differential cross sections in the  $k_T$ -factorization approach and describe the unintegrated gluon distributions which we use in our calculations.

### 2.1 Kinematics

As indicated in Fig. 1, we denote the 4-momenta of the incoming protons and the outgoing heavy quarks as  $k_1$ ,  $k_2$  and  $p_1$ ,  $p_2$ , respectively. The initial gluons have the 4-momenta  $q_1$  and  $q_2$ . We use the Sudakov decomposition, which has the form

$$\begin{aligned} p_1 &= \alpha_1 k_1 + \beta_1 k_2 + p_{1T}, & p_2 &= \alpha_2 k_1 + \beta_2 k_2 + p_{2T}, \\ q_1 &= x_1 k_1 + q_{1T}, & q_2 &= x_2 k_2 + q_{2T}, \end{aligned} \quad (2)$$

where  $p_{1T}$ ,  $p_{2T}$ ,  $q_{1T}$  and  $q_{2T}$  are the transverse (4-vector) momenta of the corresponding particles, and

$$p_1^2 = p_2^2 = m_Q^2, \quad q_1^2 = q_{1T}^2, \quad q_2^2 = q_{2T}^2. \quad (3)$$

In the  $p\bar{p}$  c.m. frame we can write:

$$k_1 = \sqrt{s}/2 (1, 0, 0, 1), \quad k_2 = \sqrt{s}/2 (1, 0, 0, -1), \quad (4)$$

where we neglect the masses of the protons. The Sudakov variables are expressed as follows:

$$\begin{aligned} \alpha_1 &= \frac{m_{1T}}{\sqrt{s}} \exp(y_1), & \alpha_2 &= \frac{m_{2T}}{\sqrt{s}} \exp(y_2), \\ \beta_1 &= \frac{m_{1T}}{\sqrt{s}} \exp(-y_1), & \beta_2 &= \frac{m_{2T}}{\sqrt{s}} \exp(-y_2), \end{aligned} \quad (5)$$

where  $m_{1,2T}^2 = m_Q^2 + p_{1,2T}^2$ , and  $y_1$  and  $y_2$  are the rapidities of final heavy quarks in the  $p\bar{p}$  c.m. frame. From the conservation laws, we can easily obtain the following conditions:

$$x_1 = \alpha_1 + \alpha_2, \quad x_2 = \beta_1 + \beta_2, \quad q_{1T} + q_{2T} = p_{1T} + p_{2T}. \quad (6)$$

## 2.2 Inclusive heavy quark production cross section

Here we recall some formulas from our previous paper [17]. In the  $k_T$ -factorization approach, the differential cross section for inclusive heavy quark production may be written as

$$d\sigma(p\bar{p} \rightarrow Q\bar{Q} X) = \frac{1}{16\pi(x_1 x_2 s)^2} \Phi(x_1, q_{1T}^2, \mu^2) \Phi(x_2, q_{2T}^2, \mu^2) \times \sum |M|_{\text{SHA}}^2(g^*g^* \rightarrow Q\bar{Q}) dy_1 dy_2 dp_{2T}^2 dq_{1T}^2 dq_{2T}^2 \frac{d\phi_1}{2\pi} \frac{d\phi_2}{2\pi} \frac{d\phi_Q}{2\pi}, \quad (7)$$

where  $\Phi(x_1, q_{1T}^2, \mu^2)$  and  $\Phi(x_2, q_{2T}^2, \mu^2)$  are the unintegrated gluon distributions in the proton,  $\phi_1, \phi_2$  and  $\phi_Q$  are the azimuthal angles of the initial gluons and final heavy quark respectively,  $\sum |M|_{\text{SHA}}^2(g^*g^* \rightarrow Q\bar{Q})$  is the off-mass-shell matrix element. Symbol  $\sum$  in Equ. (7) indicates the averaging over the initial and the summation over the final polarization states. The expression for the  $\sum |M|_{\text{SHA}}^2(g^*g^* \rightarrow Q\bar{Q})$  was obtained in our previous paper [17].

Formulas for the differential cross sections in the standard parton model (SPM) may be obtained from Equ. (7) if we take the limit  $q_{1,2T}^2 \rightarrow 0$  and average over the transverse momentum vector  $q_{1,2T}$ :

$$d\sigma(p\bar{p} \rightarrow Q\bar{Q} X) = \frac{1}{16\pi(x_1 x_2 s)^2} x_1 G(x_1, \mu^2) x_2 G(x_2, \mu^2) \times \sum |M|_{\text{PM}}^2(gg \rightarrow Q\bar{Q}) dy_1 dy_2 dp_{1T}^2 \frac{d\phi_Q}{2\pi}, \quad (8)$$

where  $\sum |M|_{\text{PM}}^2(gg \rightarrow Q\bar{Q})$  is the gluon-gluon fusion matrix element obtained in the standard parton model.

## 2.3 Unintegrated gluon distributions

Various parametrizations of the unintegrated gluon distribution used in our calculations are discussed below (see also [23]).

As the first set, we use a BFKL-like parametrization (hereafter denoted as the JB parametrization) given in [24]. The method proposed in [24] lies upon a straightforward perturbative solution of the BFKL equation where collinear gluon density  $xG(x, \mu^2)$  is used as the boundary condition. The unintegrated gluon distribution is calculated as a convolution of collinear gluon distribution  $xG(x, \mu^2)$  with universal weight factors:

$$\Phi(x, q_T^2, \mu^2) = \int_x^1 \varphi(\eta, q_T^2, \mu^2) \frac{x}{\eta} G\left(\frac{x}{\eta}, \mu^2\right) d\eta, \quad (9)$$

where

$$\varphi(\eta, q_T^2, \mu^2) = \begin{cases} \frac{\bar{\alpha}_S}{\eta q_T^2} J_0\left(2\sqrt{\bar{\alpha}_S \ln(1/\eta) \ln(\mu^2/q_T^2)}\right), & \text{if } q_T^2 \leq \mu^2, \\ \frac{\bar{\alpha}_S}{\eta q_T^2} I_0\left(2\sqrt{\bar{\alpha}_S \ln(1/\eta) \ln(q_T^2/\mu^2)}\right), & \text{if } q_T^2 > \mu^2, \end{cases} \quad (10)$$

where  $J_0$  and  $I_0$  stand for Bessel functions of real and imaginary arguments respectively, and  $\bar{\alpha}_S = 3\alpha_S/\pi$ . In calculations we used the standard GRV set [25] for  $xG(x, \mu^2)$ . The parameter  $\bar{\alpha}_S$  is connected with the Pomeron trajectory intercept:  $\Delta = 4\bar{\alpha}_S \ln 2$  in the LO,

and  $\Delta = 4\bar{\alpha}_S \ln 2 - N\bar{\alpha}_S^2$  in the NLO approximations, where  $N \sim 18$  [26, 27]. The latter value of  $\Delta$  could have dramatic consequences on the high energy phenomenology. However, some resummation procedures proposed in the last years lead to positive values:  $\Delta \sim 0.2 - 0.3$  [27, 28]. The result  $\Delta = 0.35$  was obtained from the description of the  $p_T$  spectrum of  $D^*$  mesons in the electroproduction at HERA [29]. We use this value of the parameter  $\Delta$  in the present paper<sup>4</sup>.

Another set of unintegrated gluon densities (the KMS parametrization) [30] is obtained from a unified BFKL and DGLAP description of  $F_2$  data and includes the so called consistency constraint [31]. The consistency constraint introduces a large correction to the LO BFKL equation: about 70% of the full NLO corrections to the BFKL exponent  $\Delta$  are effectively included in this constraint, as is explained in [32].

Finally, the third unintegrated gluon function used here is the one which is obtained from conventional gluon density  $xG(x, \mu^2)$  by taking the  $\mu^2$ -derivative [7, 11, 33]:

$$\Phi(x, q_T^2) = \left. \frac{d xG(x, \mu^2)}{d\mu^2} \right|_{\mu^2=q_T^2}. \quad (11)$$

Here we have used the expression for  $xG(x, \mu^2)$  from the standard GRV set [25]. We point out that the parametrization (11), in contrast with JB and KMS parametrizations, takes into account the terms  $\alpha_S^n \ln^n(\mu^2/\Lambda_{\text{QCD}}^2)$  and  $\alpha_S^n \ln^n(\mu^2/\Lambda_{\text{QCD}}^2) \ln^n(1/x)$  only. It is interesting to compare the numerical results obtained with the parametrizations JB and (11) because they are derived from the same collinear density but underwent evolution according to different (BFKL or DGLAP) equations.

The integration limits in (7) and (8) are given by the kinematic conditions of the D $\odot$  and CDF experiments [1–5]. The calculation of the heavy quark production cross section in the  $k_T$ -factorization approach have been done according to (7) for  $q_{1T}^2 \geq Q_0^2$  and  $q_{2T}^2 \geq Q_0^2$ . For the regions  $q_{1T}^2 \leq Q_0^2$  and  $q_{2T}^2 \leq Q_0^2$ , we set  $q_{1T}^2 = 0$  and  $q_{2T}^2 = 0$  in the matrix elements of the hard subprocesses, take  $\sum |M|_{\text{PM}}^2(gg \rightarrow Q\bar{Q})$  instead of  $\sum |M|_{\text{SHA}}^2(g^*g^* \rightarrow Q\bar{Q})$  and use equation (8) of the usual parton model. The contributions from the asymmetric configurations ( $q_{1T}^2 \leq Q_0^2$ ,  $q_{2T}^2 \geq Q_0^2$  and  $q_{1T}^2 \geq Q_0^2$ ,  $q_{2T}^2 \leq Q_0^2$ ) are included in a similar way, where one of the gluons is described by the unintegrated distribution and the other one by the collinear density. The choice of the critical value of the parameter  $Q_0^2 = 1 \text{ GeV}^2$  is determined by the requirement that the value of  $\alpha_S(\mu^2)$  in the region  $q_{1,2T}^2 \geq Q_0^2$  be small (where in fact  $\alpha_S(\mu^2) < 0.26$ ).

### 3 Numerical results

In this section we present the numerical results of our calculations and compare them with the D $\odot$  [4, 5], CDF [1–3] and UA1 [34] data.

Besides the choice of the unintegrated gluon distribution, our theoretical results depend on the bottom quark mass, the factorization scale  $\mu^2$  and the  $b$  quark fragmentation function. For example, a special choice of the  $b$ -quark fragmentation function was used in paper [6] as a way to increase the  $B$ -meson production cross section in observable region of transverse momentum. In the present paper we convert  $b$  quarks into  $B$ -mesons using the usual Peterson

<sup>4</sup>We also used this value of  $\Delta$  in the analysis of experimental data on the  $J/\psi$  photo- and leptonproduction at HERA [19, 20] and in the description [21, 22] of deep inelastic structure functions  $F_2^c$ ,  $F_L^c$  and  $F_L$  in the small  $x$  region.

fragmentation function [35] with  $\epsilon = 0.006$ . Regarding the other parameters, we use  $m_b = 4.75$  GeV and  $\mu^2 = q_{1,2T}^2$  as in [8, 14]<sup>5</sup>.

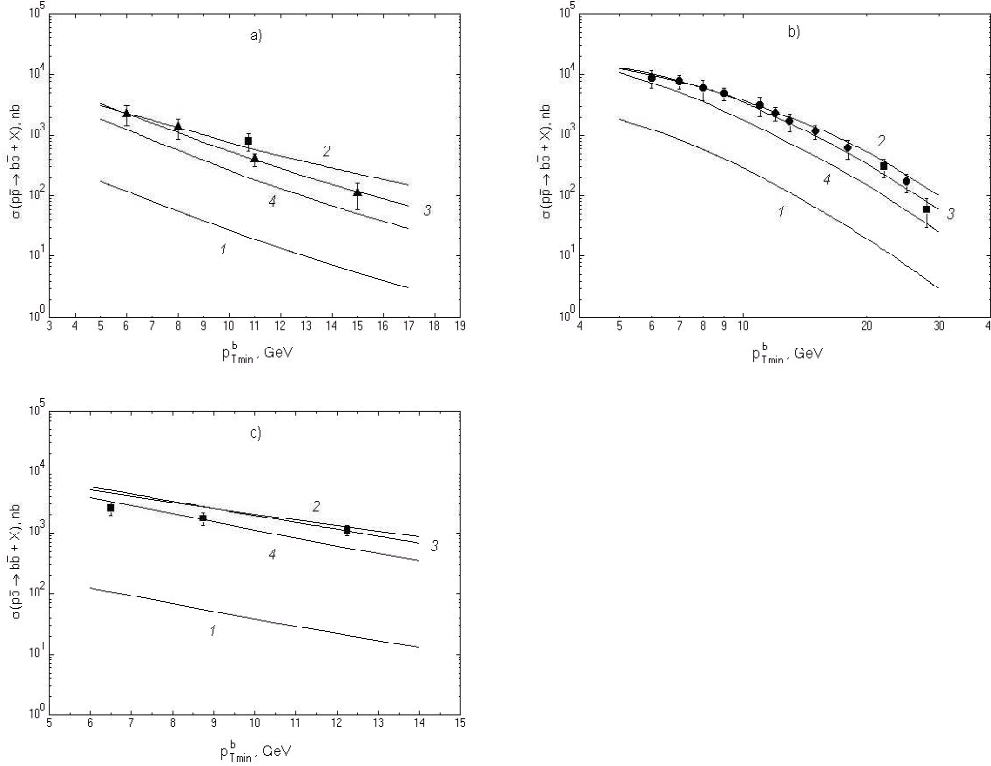


Figure 2: The  $b$  quark transverse momentum distributions at Tevatron conditions presented in the form of integrated cross sections. The cuts applied:  $|y_1| < 1.5$ ,  $|y_2| < 1.5$ ,  $\sqrt{s} = 630$  GeV (Fig. 2a),  $|y_1| < 1$ ,  $\sqrt{s} = 1800$  GeV (Fig. 2b) and  $|y_1| < 1$ ,  $|y_2| < 1$ ,  $\sqrt{s} = 1800$  GeV (Fig. 2c). Curve 1 corresponds to the SPM calculations in the leading order approximation with GRV (LO) gluon density, curves 2, 3 and 4 correspond to the  $k_T$ -factorization results with JB, KMS and Equ. (11) unintegrated gluon distributions. Experimental data are from UA1 [34]  $\blacktriangle$ , D0 [5]  $\bullet$  and CDF [3]  $\blacksquare$ .

The results of our calculations are shown in Fig. 2–9. Fig. 2 displays the  $b$  quark transverse momentum distribution at Tevatron conditions presented in the form of integrated cross sections. The following cuts were applied:  $|y_1| < 1.5$ ,  $|y_2| < 1.5$ ,  $\sqrt{s} = 630$  GeV (Fig. 2a),  $|y_1| < 1$ ,  $\sqrt{s} = 1800$  GeV (Fig. 2b) and  $|y_1| < 1$ ,  $|y_2| < 1$ ,  $\sqrt{s} = 1800$  GeV (Fig. 2c). Curve 1 corresponds to the SPM calculations at the leading order approximation with the GRV (LO) gluon density, curves 2, 3 and 4 correspond to the  $k_T$ -factorization results with the JB, KMS and the (11) unintegrated gluon distributions, respectively. One can see that the results obtained in the  $k_T$ -factorization approach agree very well with the D0 and CDF experimental data. The calculations based on the parametrization (11), which takes into account only the terms  $\alpha_S^n \ln^n(\mu^2/\Lambda_{\text{QCD}}^2)$  and  $\alpha_S^n \ln^n(\mu^2/\Lambda_{\text{QCD}}^2) \ln^n(1/x)$  predict the cross section which is lower than the data by a factor of about 2 (Fig. 2a and Fig. 2b). We would like to note the difference in the shapes between the curves obtained using the

<sup>5</sup>We also used this choice of  $\mu^2$  earlier [19, 20] for the description of  $J/\psi$  photo- and leptonproduction processes at HERA within the  $k_T$ -factorization approach and the colour singlet model.

$k_T$ -factorization approach and the standard parton model. This difference shows the  $p_T$  broadening effect which is usual for the  $k_T$ -factorization approach. At the same time, the shape of the curves 4 and 1 is practically identical.

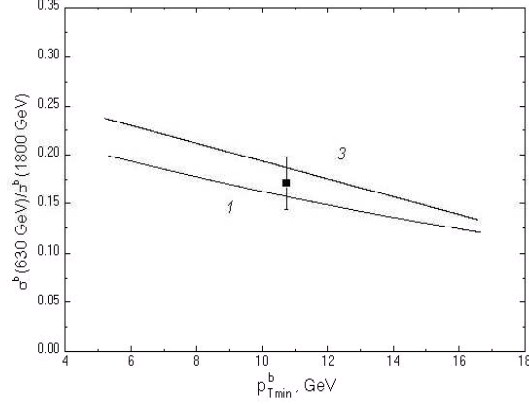


Figure 3: The ratio of  $\sigma(b)$  at  $\sqrt{s} = 630$  GeV to  $\sqrt{s} = 1800$  GeV as a function of the minimum  $b$  quark transverse momentum  $p_{T\min}^b$ . Notation of the curves 1 and 3 is the same as in Fig. 2. Experimental data are from CDF[1] ■.

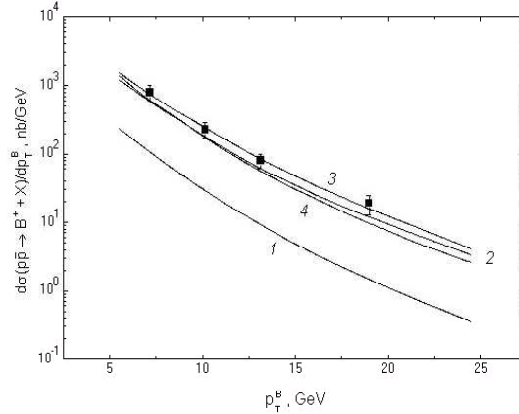


Figure 4: Theoretical predictions for the  $B$  meson  $p_T$  spectrum at  $\sqrt{s} = 1800$  GeV compared to the CDF data. The cuts applied:  $|y^B| < 1$ . Notation of the curves 1 — 4 is the same as in Fig. 2. Experimental data are from CDF [2] ■.

It is notable that, in the collinear approximation, the sum of the LO and NLO pQCD contributions still underestimates the  $b$  quark production rate by a factor of 2 [3, 5]. The results obtained in the  $k_T$ -factorization approach in Ref. [16] lie above the sole LO contribution, but below the sum of LO and NLO contributions, in an apparent disagreement with our present results. The roots of this discrepancy are connected with the parameter settings accepted in Ref. [16], that is, the large values of the quark mass  $m_b = 5$  GeV and the renormalization

scale  $\mu^2 = m_{1,2T}^2$  in the running coupling constant.

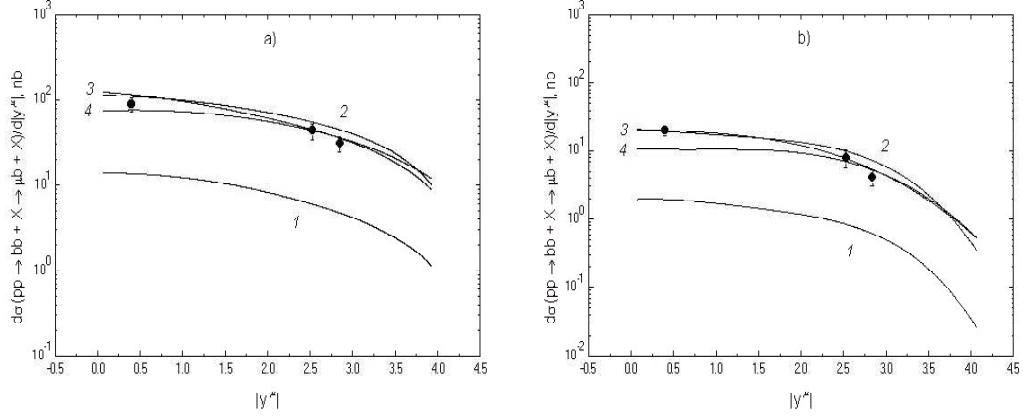


Figure 5: The cross section for muons from  $B$  meson decay as a function of rapidity compared to the  $D\circlearrowleft$  data. The cuts applied:  $p_T^\mu > 5$  GeV (Fig. 5a) and  $p_T^\mu > 8$  GeV (Fig. 5b). Notation of the curves 1 — 4 is the same as in Fig. 2. Experimental data are from  $D\circlearrowleft$  [4] ●.

Fig. 3 shows the ratio of the cross sections measured at different beam energies,  $\sigma(b)$  at  $\sqrt{s} = 630$  GeV to  $\sqrt{s} = 1800$  GeV, as a function of the minimum  $b$  quark transverse momentum  $p_{T\min}^b$ . Notation of the curves 1, 3 is the same as in Fig. 2. One can see that the experimental data collected by the  $D\circlearrowleft$  collaboration agree with the LO pQCD calculations as well as with the  $k_T$ -factorization ones. This result is not surprising because, when the ratio of the cross sections is considered, many factors affecting the absolute normalization, as well as many theoretical and experimental uncertainties partially or completely cancel out [1].

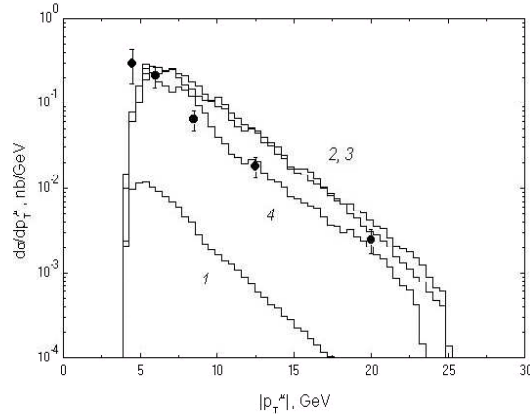


Figure 6: Predictions on the leading muon  $p_T$  spectrum in the  $b\bar{b}$  production events compared to the  $D\circlearrowleft$  data. The cuts applied to both muons:  $4 < p_T^\mu < 25$  GeV,  $|\eta^\mu| < 0.8$  and  $6 < m^{\mu\mu} < 35$  GeV. Notation of the histograms 1 — 4 is the same as in Fig. 2. Experimental data are from  $D\circlearrowleft$  [5] ●.



Fig. 4 shows the prediction for the  $B$  meson  $p_T$  spectrum at  $\sqrt{s} = 1800$  GeV compared to the CDF data [3] within the experimental cuts  $|y^B| < 1$ . Notation of the curves 1 — 4 is the same as in Fig. 2. Here we find good agreement between the results obtained in the  $k_T$ -factorization approach and experimental data. One can see that the  $p_T$  broadening effect mentioned earlier appears to be not as much clear for the  $B$  meson production as it was for the  $b$  quark production. This is because of compensatory effects in the fragmentation process. We note again that the ordinary NLO pQCD calculations underestimate the  $B$  meson production by a factor of 3 [2].

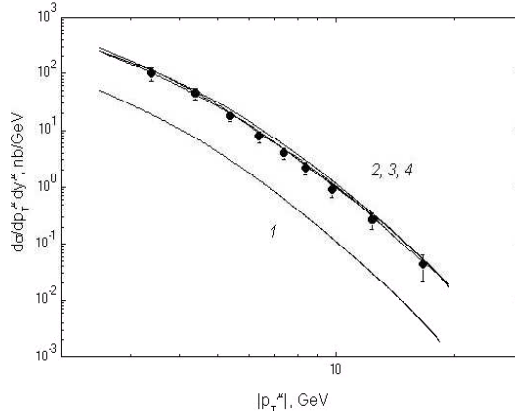


Figure 7: Double differential cross section for muons from  $B$  meson decay as a function of  $p_T^\mu$  compared to the  $D\phi$  data [4]. The cuts applied:  $2.4 < |y^\mu| < 3.2$ . Notation of the curves 1 — 4 is the same as in Fig. 2. Experimental data are from  $D\phi$  [4] ●.

The recent  $D\phi$  experimental data refer also to muons originating from semileptonic decays of  $B$ -mesons. To produce muons from  $B$ -mesons in theoretical calculations, we simulate their semileptonic decay according to the standard electroweak theory. In Fig. 5 we show the rapidity distribution  $d\sigma/d|y^\mu|$  of the decay muons for both  $p_T^\mu > 5$  GeV (Fig. 5a) and  $p_T^\mu > 8$  GeV (Fig. 5b). Notation of the curves 1 — 4 is the same as in Fig. 2. We find that the  $k_T$ -factorization results agree very well with the  $D\phi$  experimental data. In the central rapidity range  $|y^\mu| < 1$ , the results based on the parametrization Equ. (11) lie below the ones based on JB and KMS parametrizations by a factor of about 1.5. The ordinary NLO pQCD calculations lie below the data by a factor of about 4 [4].

Fig. 6 shows the leading muon  $p_T$  spectrum in the  $b\bar{b}$  production events compared to the  $D\phi$  data, where the leading muon is defined as the muon with the greatest  $p_T^\mu$  value. The cuts applied to both muons are  $4 < p_T^\mu < 25$  GeV,  $|\eta^\mu| < 0.8$  and  $6 < m^{\mu\mu} < 35$  GeV. Notation of the histograms 1 — 4 is the same as in Fig. 2. One can see that the histograms 2 and 3 lie even a bit higher than the experimental data.

The double differential cross sections  $d\sigma/dp_T^\mu dy^\mu$  in the forward rapidity region  $2.4 < |y^\mu| < 3.2$  are also well described by the  $k_T$ -factorization approach (Fig. 7). Notation of the curves 1 — 4 is the same as in Fig. 2. It is interesting to note that the shape of all the curves is practically the same. The NLO pQCD calculations underestimate the  $D\phi$  data by a factor of 4 [4].

We point out that the investigations of  $b\bar{b}$  correlations such as the azimuthal opening

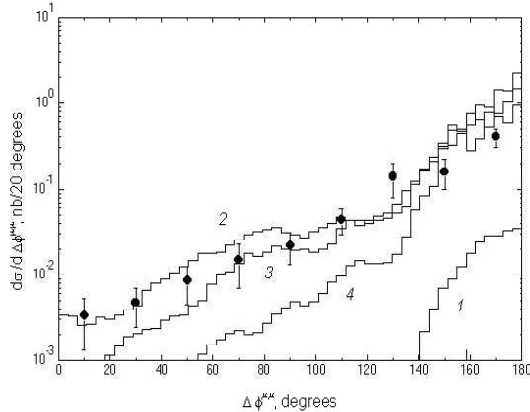


Figure 8: Azimuthal muon-muon correlations at Tevatron conditions. The cuts applied to both muons:  $4 < p_T^\mu < 25$  GeV,  $|\eta^\mu| < 0.8$  and  $6 < m^{\mu\mu} < 35$  GeV. Notation of the histograms 1 — 4 is the same as in Fig. 2. Experimental data are from  $D\otimes$  [4] ●.

angle between the  $b$  and  $\bar{b}$  quarks (or between their decay muons) allow additional details of the  $b$  quark production to be tested since these quantities are sensitive to the relative contributions of the different production mechanisms [8, 12–14, 16]. In the naive gluon-gluon fusion mechanism, the distribution over the azimuthal angle difference  $\Delta\phi^{b\bar{b}}$  must be simply a delta function  $\delta(\Delta\phi^{b\bar{b}} - \pi)$ . Taking into account the non-vanishing initial gluon transverse momenta  $q_{1T}$  and  $q_{2T}$  leads to the violation of this back-to-back quark production kinematics in the  $k_T$ -factorization approach.

The differential  $b\bar{b}$  cross section  $d\sigma/d\Delta\phi^{\mu\mu}$  is shown in Fig. 8. The cuts applied to both muons are  $4 < p_T^\mu < 25$  GeV,  $|\eta^\mu| < 0.8$  and  $6 < m^{\mu\mu} < 35$  GeV. Notation of the histograms 1 — 4 is the same as in Fig. 2. One can see that good agreement between JB and KMS predictions and the experimental data is observed. The shape of the histogram 4 strongly differs from that of the histograms 2 and 3. In the small  $\Delta\phi^{\mu\mu} \sim 0$  region, the parametrization (11) underestimates the  $D\otimes$  experimental data. This fact indicates the importance of the large  $\alpha_S^n \ln^n(1/x)$  contributions. One can see that the properties of different unintegrated gluon distributions manifest themselves in the  $b\bar{b}$  or muon-muon azimuthal correlations. As expected, the sole LO pQCD contribution predicts a peak at  $\Delta\phi^{\mu\mu} \sim \pi$ .

In addition, we present our predictions for muon-muon (Fig. 9a) and muon-jet (Fig. 9b) cross sections at the Tevatron and CERN LHC conditions. In the latter case, we take the kinematic requirements of the detector ATLAS [36] as a representative example. This conditions imply the presence of a decay muon with  $p_T^\mu > 6$  GeV and  $|y^\mu| < 2.5$ . Curves 1 — 4 are the same as in Fig. 2. We point out that the predicted cross sections are rather uncertain and approximate because we neglected the saturation effects in the gluon distributions [8, 12, 13]. However, the threshold value of  $x$  (where these effects will come into play) is still unknown.

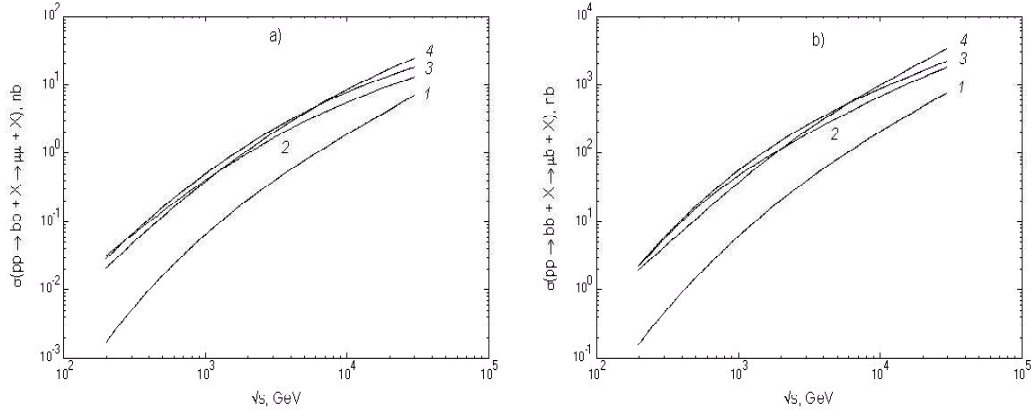


Figure 9: Theoretical predictions for muon-muon (Fig. 9a) and muon-jet (Fig. 9b) cross sections as functions of  $\sqrt{s}$  at the Fermilab Tevatron and CERN LHC conditions. The cuts applied:  $p_T^\mu > 6$  GeV,  $|y^\mu| < 2.5$ . Notation of the curves 1 — 4 is the same as in Fig. 2.

## 4 Conclusions

In this paper we have considered heavy quark production in  $p\bar{p}$  collisions at Tevatron in the framework of the  $k_T$ -factorization approach. We investigated the dependence of the  $b$  quark,  $B$  meson and the decay muon cross sections on different forms of the unintegrated gluon distribution. The analysis covered the azimuthal correlations between the  $b$  and  $\bar{b}$  quarks and their decay muons. We compared the theoretical results with recent experimental data collected by the DØ and CDF collaborations at Tevatron. We found that the  $k_T$ -factorization results agree well with the experimental data when we use JB or KMS unintegrated gluon distributions and set the quark mass  $m_b = 4.75$  GeV, the factorization scale  $\mu^2 = q_T^2$  and  $\Lambda_{\text{QCD}} = 250$  MeV. The properties of different unintegrated gluon distributions manifest themselves in the  $b\bar{b}$  or muon-muon azimuthal correlations. From the analysis of these correlations we can conclude that JB and KMS unintegrated gluon distributions are more preferable than the parametrization (11). Finally, we present our predictions for the muon-muon and muon-jet cross sections at Tevatron and CERN LHC conditions.

## 5 Acknowledgments

The study was supported in part by RFBR grant N° 02–02–17513. A.V.L. also was supported by INTAS grant YSF 2002 N° 399.

## References

- [1] D. Acosta *et al.* (CDF Collab.), hep-ex/0206019.
- [2] D. Acosta *et al.* (CDF Collab.), Phys. Rev. D **65**, 052005 (2002).

- [3] F. Abe *et al.* (CDF Collab.), Phys. Rev. D **55**, 2546 (1997).
- [4] B. Abbott *et al.* (D $\phi$  Collab.), hep-ex/9907029.
- [5] B. Abbott *et al.* (D $\phi$  Collab.), Phys. Lett. B **487**, 264 (2000); hep-ex/9905024.
- [6] M. Cacciari and P. Nason, hep-ph/0204025.
- [7] L.V. Gribov, E.M. Levin and M.G. Ryskin, Phys. Rep. **100**, 1 (1983).
- [8] E.M. Levin, M.G. Ryskin, Yu.M. Shabelsky and A.G. Shuvaev, Yad. Fiz. **53**, 1059 (1991).
- [9] S. Catani, M. Ciafaloni and F. Hautmann, Nucl. Phys. B **366**, 135 (1991).
- [10] J.C. Collins and R.K. Ellis, Nucl. Phys. B **360**, 3 (1991).
- [11] E.A. Kuraev, L.N. Lipatov and V.S. Fadin, Sov. Phys. JETP **44**, 443 (1976); **45**, 199 (1977);  
Yu.Yu. Balitsky and L.N. Lipatov, Sov. J. Nucl. Phys. **28**, 822 (1978).
- [12] M.G. Ryskin and Yu.M. Shabelski, Z. Phys. C **69**, 269 (1996).
- [13] M.G. Ryskin, Yu.M. Shabelski and A.G. Shuvaev, Phys. Atom. Nucl. **64**, 1995-2005 (2001); hep-ph/990757; hep-ph/0007238.
- [14] P. Hägler, R. Kirschner, A. Schafer *et al.*, Phys. Rev. D **62**, 071502 (2000).
- [15] H. Jung, Phys. Rev. D **65**, 034015 (2002); hep-ph/0110034.
- [16] S.P. Baranov and M. Smizanska, Phys. Rev. D **62**, 014012 (2000).
- [17] A.V. Lipatov, V.A. Saleev and N.P. Zotov, Yad. Fiz. **66**, 1 (2003); hep-ph/0112114; in *Proceedings of the QFTHEP'2001*, Moscow, Russia, 2002, p. 238.
- [18] V.A. Saleev and N.P. Zotov, Mod. Phys. Lett. A **9**, 151 (1994); A **11**, 25 (1996);  
A.V. Lipatov and N.P. Zotov, Mod. Phys. Lett. A **15**, 695 (2000);  
A.V. Lipatov, V.A. Saleev and N.P. Zotov, Mod. Phys. Lett. A **15**, 1727 (2000).
- [19] A.V. Lipatov and N.P. Zotov, to be published in Yad. Fiz. (2003); hep-ph/0208237.
- [20] A.V. Lipatov and N.P. Zotov, to be published in Eur. Phys. J. C (2003); hep-ph/0210310.
- [21] A.V. Kotikov, A.V. Lipatov, G. Parente and N.P. Zotov, Eur. Phys. J. C **26**, 51 (2002).
- [22] A.V. Kotikov, A.V. Lipatov and N.P. Zotov, to be published in Eur. Phys. J. C (2003), hep-ph/0207226.
- [23] B. Andersson *et al.* (Small  $x$  Collab.), Eur. Phys. J. C **25**, 77 (2002).
- [24] J. Blümlein, DESY 95-121.
- [25] M. Glück, E. Reya and A. Vogt, Z. Phys. C **67**, 433 (1995).
- [26] V.S. Fadin and L.N. Lipatov, Phys. Lett. B **429**, 127 (1998);  
M. Ciafaloni and G. Camici, Phys. Lett. B **430**, 349 (1998).

- [27] G. Salam, JHEP **9807:019** (1998); hep-ph/9806482.
- [28] S.J. Brodsky, V.S. Fadin, V.T. Kim, L.N. Lipatov and G.B. Pivovarov, JETP Lett.**70**, 155 (1999).
- [29] S.P. Baranov and N.P. Zotov, Phys. Lett. B **458**, 389 (1999); B **491**, 111 (2000).
- [30] J. Kwiecinski, A.D. Martin and A.M. Stasto, Phys. Rev. D **56**, 3991 (1997).
- [31] J. Kwiecinski, A.D. Martin and A.M. Sutton, Phys. Rev. D **52**, 1445 (1995); Z. Phys. C **71**, 585 (1996).
- [32] J. Kwiecinski, A.D. Martin and J.J. Outhwaite, Eur. Phys. J. C **9**, 611 (2001).
- [33] N.N. Nikolaev and B.G. Zakharov, Phys. Lett. B **333**, 250 (1994).
- [34] C. Albajar *et al.*, Z. Phys. C **61**, 41 (1994).
- [35] K.A. Peterson, D. Schlatter, I. Schmitt and P.M. Zerwas, Phys. Rev. D **27**, 105 (1983).
- [36] W. Armstrong *et al.* (ATLAS Collab.), CERN/LHCC/94-43.